One- and two-dimensional photo-imprinted diffraction gratings for manipulating terahertz waves

Ioannis Chatzakis,[1,a)] Philippe Tassin,[1,b)] Liang Luo,[1] Nian-Hai Shen,[1] Lei Zhang,[1] Jigang Wang,[1,c)] Thomas Koschny,[1] and C. M. Soukoulis[1,2,d)]
[1]*Ames Laboratory—U.S. DOE and Department of Physics and Astronomy, Iowa State University, Ames, Iowa 50011, USA*
[2]*Institute of Electronic Structure and Lasers (IESL), FORTH, 71110 Heraklion, Crete, Greece*

(Received 8 May 2013; accepted 6 June 2013; published online 22 July 2013)

Emerging technology based on artificial materials containing metallic structures has raised the prospect for unprecedented control of terahertz waves. The functionality of these devices is static by the very nature of their metallic composition, although some degree of tunability can be achieved by incorporating electrically biased semiconductors. Here, we demonstrate a photonic structure by projecting the optical image of a metal mask onto a thin GaAs substrate using a femtosecond pulsed laser source. We show that the resulting high-contrast pattern of photo-excited carriers can create diffractive elements operating in transmission, potentially providing a route to terahertz components with reconfigurable functionality. © *2013 AIP Publishing LLC*.
[http://dx.doi.org/10.1063/1.4813620]

The terahertz spectral range of the electromagnetic spectrum—loosely defined from about 100 GHz to 10THz—has long been an inaccessible region in between the successful realms of electronics and photonics, because of the lack of efficient and compact sources and detectors for terahertz radiation. In the past few decades, however, the development of technologies like quantum-cascade lasers,[1–3] terahertz wave generation through nonlinear crystals[4] and terahertz time-domain spectroscopy[5,6] has enabled the exploration of terahertz science and the rapid rise of terahertz imaging and spectroscopy for, amongst others, biomedical and security applications.[7,8] Controlling terahertz radiation has proven to be more difficult, although recent breakthroughs in waveguiding[9] and manipulating[10–15] terahertz waves have been reported. A major driving force behind these breakthroughs is the progress that scientists have made in artificial materials containing conductive structures, for example, frequency-selective surfaces,[16] metamaterials[17–19] and photonic crystals.[20–22] By carefully tailoring the response of these artificial materials, it is possible to create terahertz devices like filters,[10,11] absorbers,[12,13] and polarizers.[14,15] It is even possible to achieve tunability by incorporating semiconductors with electrical biasing into the artificial materials[23–25] or the ability to switch between two different states,[26–29] but these devices have essentially a specific functionality determined at the time of their design.

In this letter, we develop an approach for a reconfigurable terahertz component, which can be switched between a wide class of functionalities, such as beam shaping, beam steering, and wavefront correction. The foundation of this approach, which is based on diffraction gratings, is the experiment outlined in Fig. 1.[30] An 800 nm femtosecond-pulsed laser beam[31–33] illuminates a metal mask and the image of the mask is projected with a lens onto a 1-mm-thin GaAs substrate. This creates a pattern of illuminated and dark regions on the substrate as shown in the inset of Fig. 1. Where illuminated, the pump beam creates carriers in the substrate by photo-excitation and the result is a photo-imprinted conductive pattern of free carriers inside the GaAs substrate, which we can use to manipulate terahertz waves. Being made from a copper film that is essentially impenetrable to the pump beam, the metal mask enables us in principle to create high-contrast light patterns on the GaAs substrate only limited by diffraction of the optical pump beam.

We subsequently show that the resulting photo-imprinted patterns can be used as diffractive elements for terahertz waves operating in transmission, which is highly desirable for many applications. Terahertz pulses, generated by

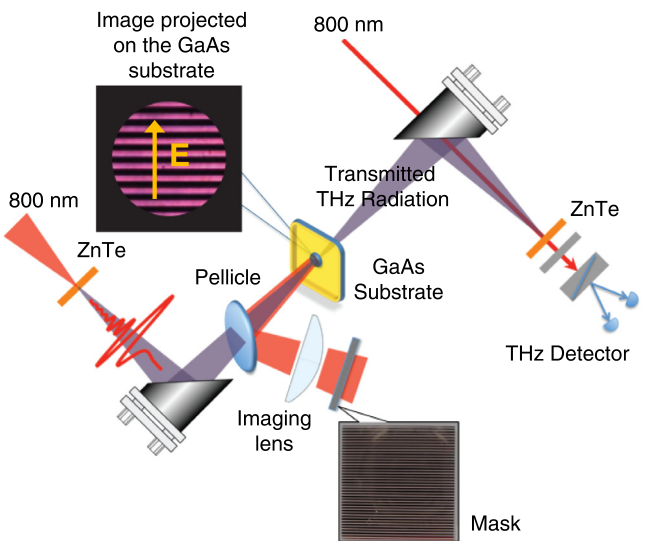

FIG. 1. The experimental setup providing the basis for reconfigurable diffractive elements for terahertz waves. Optically projecting a mask on a GaAs substrate creates a grating in carrier concentration in the surface layer of the substrate.

[a)]Present address: Department of Materials Science and Engineering, Stanford University, Stanford, California 94305, USA.
[b)]Author to whom correspondence should be addressed: Electronic mail: tassin@ameslab.gov
[c)]Electronic mail: jgwang@iastate.edu, jwang@ameslab.gov
[d)]Electronic mail: soukoulis@ameslab.gov

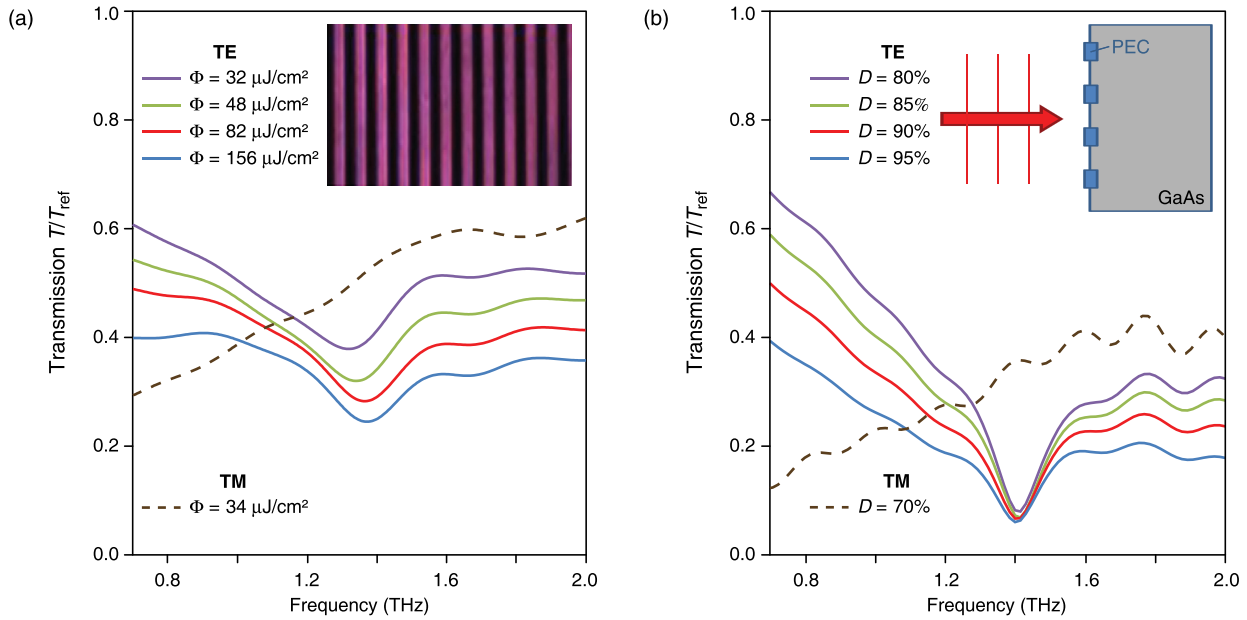

FIG. 2. Terahertz transmission spectra of the photo-imprinted linear grating. (a) Experimental transmission spectra of a grating (lattice constant $a = 60\,\mu$m) with duty cycle $D = 50\%$ for several pump fluencies. The inset shows the projected image of the metal mask at the position of the sample measured with a CCD camera. (b) Simulation results from a simplified model of a diffraction grating (lattice constant $a = 60\,\mu$m) consisting of PEC wires for different duty cycles D.

optical rectification of the femtosecond laser pulses in a ZnTe crystal, are focused on the GaAs sample and the transmitted terahertz waves are detected by means of electro-optic sampling in a second ZnTe crystal. The terahertz pulse duration is approximately 2 ps, which is much smaller than the recombination time ($\approx$1ns) and the diffusion time (in 1 ns the carriers diffuse over a distance less than 2 μm) of the photocarriers, so the photo-imprinted grating can be considered to be essentially static for a single terahertz pulse. We start with a copper mask creating a photo-imprinted linear grating with lattice constant of 60 μm and a duty cycle of $D = 50\%$. From the terahertz transmission spectra for a set of different pump fluences, shown in Fig. 2(a), we observe a pronounced spectral feature with strongly reduced transmission at about $f = 1.39$ THz when the electric field is polarized perpendicular to the grating lines (TE). For the other polarization (TM), no sharp spectral feature is observed. We also observe higher background transmission levels for low pump fluence—i.e., when few photocarriers are created—and low background transmission for higher pump fluence.

The two most plausible mechanisms possibly behind the spectral feature are (i) coupling to the first diffraction order in GaAs and (ii) a quasistatic electric dipole resonance in the cut-wire elements created by the neighboring stripes of the grating. In order to distinguish between both mechanisms, we have fabricated a set of masks with varying lattice constant (duty cycle fixed at $D = 50\%$) and a set with varying duty cycle (lattice constant fixed at $a = 60\,\mu$m). The transmission spectra for the set with varying lattice constant, displayed in Fig. 3(a), show a redshift of the spectral feature for increasing lattice constant. The spectral positions are inversely proportional to the lattice constants [see inset of Fig. 3(a)] and consistent with the cut-off frequency of the first diffraction order in GaAs, $f = c/(n_{\mathrm{GaAs}}a)$, with $n_{\mathrm{GaAs}} = 3.56$ for GaAs at 1 THz. The transmission spectra for the set with varying duty cycle, displayed in Fig. 3(b), show there is no shift in spectral position when the distance between the wires is changed. This observation rules out the electric dipole resonance, which has a resonance frequency that strongly depends on the capacitance between the cut wires.[34] The redshift of the spectral minimum when the grating period is increased points to application of our structure for reconfigurable terahertz filters.

Further evidence that our photo-imprinted gratings are purely diffraction-based and do not suffer from additional complications like quasistatic resonances or surface modes comes from simulation results[30] involving a simple linear grating of perfectly conducting wires on a GaAs substrate [see Fig. 2(b)]. The resulting transmission spectra agree qualitatively with the experimental spectra [Fig. 2(a)]—both in the spectral position of the dip and the overall shape of the transmission spectra. No surface modes or quasistatic resonances are seen in the electric field distribution obtained from the computer simulations. In addition, comparison of the experimental results of Fig. 2(a) and the simple model in Fig. 2(b) tells us that different pump fluence values result in diffraction gratings with different diffraction efficiency; i.e., the pump fluence provides us with a straightforward control over the properties of the diffractive element.

Not only can we create photo-imprinted linear gratings, but we can also generate two-dimensional diffractive elements on the GaAs substrate. One example—a square-lattice pattern with islands of photocarriers—is shown in the inset of Fig. 4 (optical image of the mask obtained with a CCD camera at the sample position). The resulting transmission spectra plotted in Fig. 4 again show a clear minimum at the diffraction edge associated with coupling of energy into the first diffraction order. In fact we can create arbitrary patterns and these experiments therefore open the door to designing diffractive elements with well-established techniques from Fourier optics, which allow determining the required amplitude gratings for fairly general functions including beam

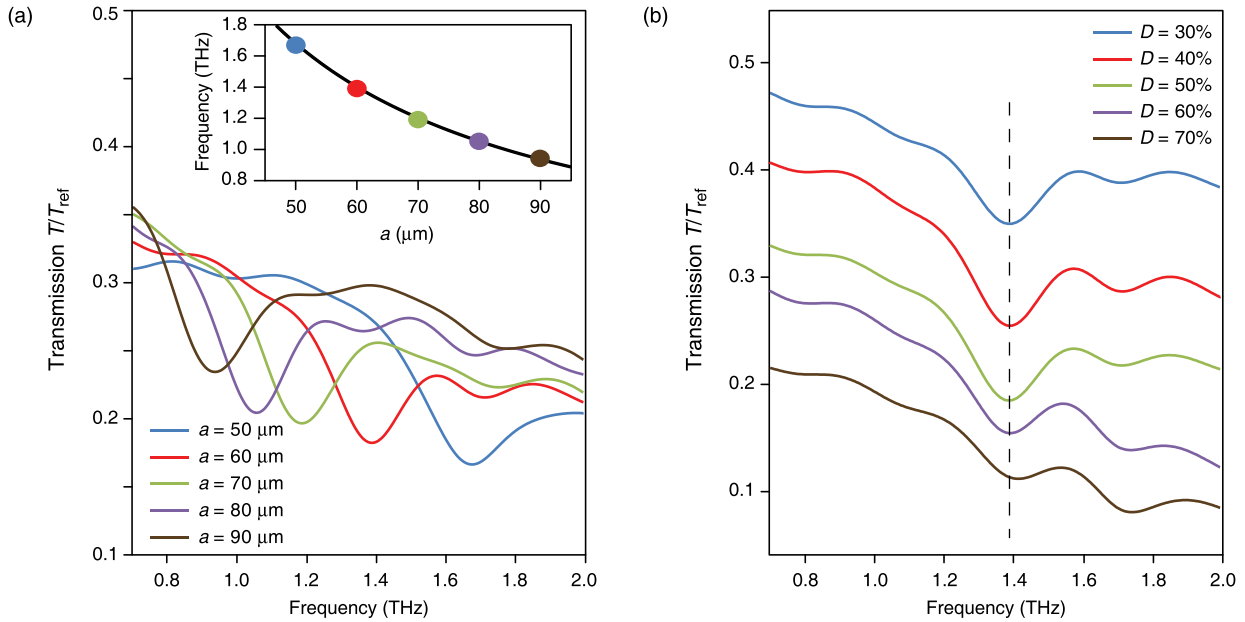

FIG. 3. (a) Experimental transmission spectra for masks with varying lattice constant (Fluence is $\Phi = 96\,\mu J/cm^2$; duty cycle is $D = 50\%$). The inset shows that the transmission dip frequencies are inversely proportional to the lattice constant (consistent with diffraction). The black line is the cut-off frequency of the first diffraction order in GaAs, $f = c/(n_{GaAs}a)$. (b) Experimental transmission spectra for masks with varying duty cycle ($\Phi = 96\,\mu J/cm^2$; $a = 60\,\mu m$). The spectral position of the dips does not depend on the duty cycle (consistent with diffraction; inconsistent with a cut-wire resonance).

shaping (Fresnel lenses, spatial filtering, wavefront correction) and beam steering, fan-outs, etc.

Finally, we performed realistic computer simulations of the experimental setup (the linear grating) that take into account the lossy nature of the photo-excited carriers.[30] We now model the photo-excited free carriers as a conductive sheet with a frequency-dependent conductivity determined from measurements of illuminated GaAs substrates without any mask in place. Fig. 5 plots the transmission spectra from these realistic simulations for several values of the carrier density—they are in excellent agreement with the experiments [Fig. 2(a)]. We accounted for the finite contrast ratio in the image of the mask. For high fluences, this results in the creation of some photocarriers in the dark regions and, thus, in diffraction gratings with finite contrast. As a consequence, we get smaller dip amplitude than in the idealized simulation of Fig. 2(b). In addition, the background transmission now depends characteristically on the carrier density (pump fluence) and the transmission dip is slightly blueshifted for higher carrier density, as observed in the experiment.

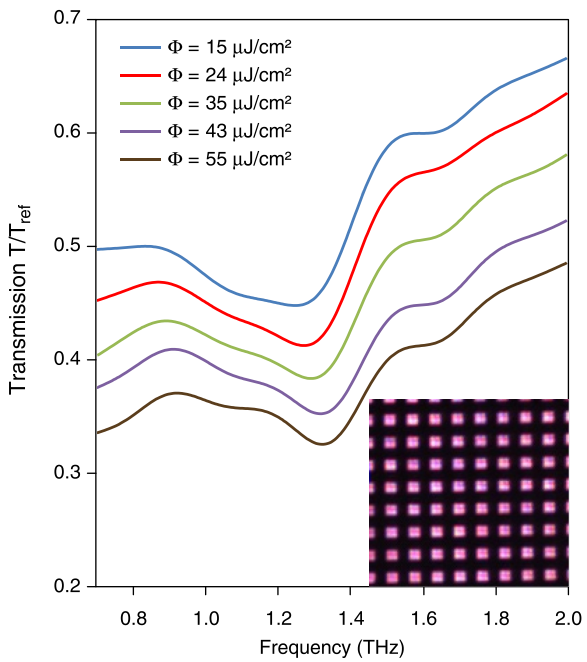

FIG. 4. Terahertz transmission spectra of a 2D photo-imprinted diffractive element. Inset: projected image of the metal mask at the position of the sample.

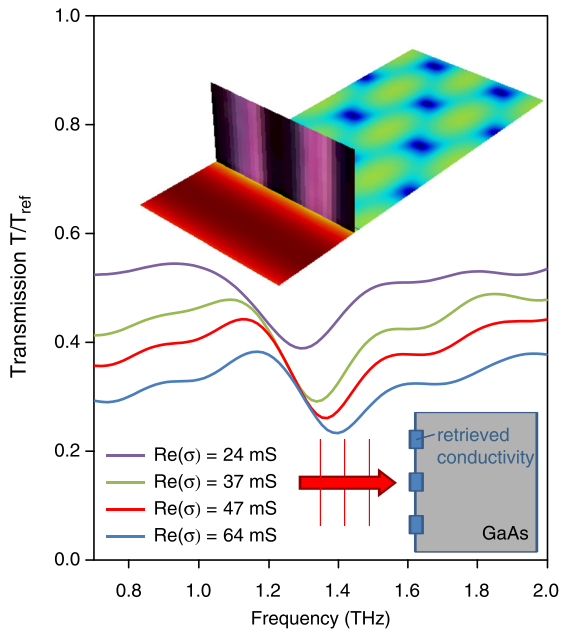

FIG. 5. Transmission spectra from computer simulations of the photo-imprinted carrier grating taking into account the lossy nature of the photo-excited carriers. (The conductivity values are specified at 1 THz.) The inset plots the electric field component perpendicular to the grating at $f = 1.6$ THz.

The inset of Fig. 5 plots the electric field inside the GaAs substrate. We observe the typical checkerboard pattern created by the interference of the transmitted and diffracted beams. We do not find any resonant fields in the structure, thus avoiding the dissipative loss that that would be produced by surface waves and resonant metamaterials.[35] The simulations described in this paragraph will also be crucial in the design of the more intricate diffractive elements mentioned above.

The demonstrated photo-imprinted diffractive elements can be made reconfigurable by replacing the fixed metal mask employed here by a device with spatially controlled transmission for the optical pump beam. One possibility is a liquid-crystal spatial light modulator as recently utilized by Okada and Tanaka[28] for tunable terahertz devices, but liquid crystals tend to have limited contrast, degrading the quality of the diffraction gratings as shown above. In order to retain the excellent contrast ratios provided by the basically impenetrable copper mask, we could replace the mask by a digital micromirror device (DMD),[36] a technology that is now widely used in DLP projection equipment. The reconfiguration rate that can be achieved in this way will be limited by the DMD mirror switching time of about 20 ms. The previous grating must also be erased, of course, but with a typical recombination time of the photocarriers of 1 ns this will not be a limiting factor. This allows for a reconfiguration rate of 50 kHz, sufficient for both sensing and imaging applications relying on terahertz science.

Work at Ames Laboratory was partially supported by the U.S. Department of Energy, Office of Basic Energy Science, Division of Materials Sciences and Engineering under Contract No. DE-AC02-07CH11358) (experiments) and by the U.S. Office of Naval Research, Award No. N00014-10-1-0925 (theory).

[1]R. Köhler, A. Tredicucci, F. Beltram, H. E. Beere, E. H. Linfield, A. G. Davies, D. A. Ritchie, R. C. Iotti, and R. Fausto, Nature **417**, 156 (2002).
[2]B. S. Williams, Nature Photon. **1**, 517 (2007).
[3]G. Scalari, C. Walther, M. Fischer, R. Terazzi, H. Beere, D. Ritchie, and J. Faist, Laser Photon. Rev. **3**, 45 (2009).
[4]K. Kawase, T. Hatanaka, H. Takahashi, K. Nakamura, T. Taniuchi, and H. Ito, Opt. Lett. **25**, 1714 (2000).
[5]M. V. Exter, C. Fattinger, and D. Grischkowsky, Opt. Lett. **14**, 1128 (1989).
[6]D. Grischkowsky, S. Keiding, M. Van Exter, and C. Fattinger, J. Opt. Soc. Am. B **7**, 2006 (1990).
[7]M. Tonouchi, Nature Photon. **1**, 97 (2007).
[8]D. Mittleman, *Sensing with Terahertz Radiation* (Springer-Verlag, Berlin, 2003).
[9]K. Wang and D. M. Mittleman, Nature **432**, 376 (2004).
[10]D. W. Porterfield, J. L. Hesler, R. Densing, E. R. Mueller, T. W. Crowe, and R. M. Weikle, Appl. Opt. **33**, 6046 (1994).
[11]H.-T. Chen, J. F. O'Hara, A. J. Taylor, R. D. Averitt, C. Highstrete, M. Lee, and W. J. Padilla, Opt. Express **15**, 1084 (2007).
[12]N. I. Landy, S. Sajuyigbe, J. J. Mock, D. R. Smith, and W. J. Padilla, Phys. Rev. Lett. **100**, 207402 (2008).
[13]M. Diem, T. Koschny, and C. M. Soukoulis, Phys. Rev. B **79**, 033101 (2009).
[14]L. Ren, C. L. Pint, T. Arikawa, K. Takeya, I. Kawayama, M. Tonouchi, R. H. Hauge, and J. Kono, Nano Lett. **12**, 787 (2012).
[15]S. Foteinopoulou, M. Kafesaki, E. N. Economou, and C. M. Soukoulis, Phys. Rev. B **84**, 035128 (2011).
[16]B. A. Munk, *Frequency Selective Surfaces: Theory and Design* (Wiley, Hoboken, 2005).
[17]D. R. Smith, J. B. Pendry, and M. C. K. Wiltshire, Science **305**, 788 (2004).
[18]C. M. Soukoulis and M. Wegener, Nature Photon **5**, 523 (2011).
[19]N. I. Zheludev and Y. S. Kivshar, Nature Mater. **11**, 917 (2012).
[20]M. M. Sigalas, C. T. Chan, K. M. Ho, and C. M. Soukoulis, Phys. Rev. B **52**, 11744 (1995).
[21]D. F. Sievenpiper, M. E. Sickmiller, and E. Yablonovitch, Phys. Rev. Lett. **76**, 2480 (1996).
[22]C. Luo, S. Johnson, J. Joannopoulos, and J. Pendry, Opt. Express **11**, 746 (2003).
[23]W. J. Padilla, A. J. Taylor, C. Highstrete, M. Lee, and R. D. Averitt, Phys. Rev. Lett. **96**, 107401 (2006).
[24]H.-T. Chen, W. J. Padilla, J. M. O. Zide, A. C. Gossard, A. J. Taylor, and R. D. Averitt, Nature **444**, 597 (2006).
[25]H.-T. Chen, J. F. O'Hara, A. K. Azad, A. J. Taylor, R. D. Averitt, D. B. Shrekenhamer, and W. J. Padilla, Nature Photon. **2**, 295 (2008).
[26]H. Tao, A. C. Strikwerda, K. Fan, W. J. Padilla, X. Zhang, and R. D. Averitt, Phys. Rev. Lett. **103**, 147401 (2009).
[27]N.-H. Shen, M. Massaouti, M. Gokkavas, J.-M. Manceau, E. Ozbay, M. Kafesaki, T. Koschny, S. Tzortzakis, and C. M. Soukoulis, Phys. Rev. Lett. **106**, 037403 (2011).
[28]T. Okada and K. Tanaka, Sci. Rep. **1**, 121 (2011).
[29]C. Kurter, P. Tassin, A. P. Zhuravel, L. Zhang, T. Koschny, A. V. Ustinov, C. M. Soukoulis, and S. M. Anlage, Appl. Phys. Lett. **100**, 121906 (2012).
[30]See supplementary material at http://dx.doi.org/10.1063/1.4813620 for the methods of the experimental and numerical analyses.
[31]T. Li, L. Luo, M. Hupalo, J. Zhang, M. C. Tringides, J. Schmalian, and J. Wang, Phys. Rev. Lett. **108**, 167401 (2012).
[32]I. Chatzakis, L. Luo, J. Wang, N.-H. Shen, T. Koschny, J. Zhou, and C. M. Soukoulis, Phys. Rev. B **86**, 125110 (2012).
[33]The laser setup is also discussed in Refs. 31 and 32.
[34]J. Zhou, E. N. Economou, T. Koschny, and C. M. Soukoulis, Opt. Lett. **31**, 3620 (2006).
[35]P. Tassin, T. Koschny, M. Kafesaki, and C. M. Soukoulis, Nature Photon. **6**, 259 (2012).
[36]S. Busch, B. Scherger, M. Scheller, and M. Koch, Opt. Lett. **37**, 1391 (2012).